RECA1-positive cells on day 21 was increased in the CD31$^-$/CD146$^-$ SP cell transplantation group compared with that in the PBS group (Fig. 3D), indicating that the transplanted cells also promote angiogenesis after ischemia. In the CD31$^-$/CD146$^-$ SP cell transplantation group (Fig. 3H), there was a decrease in cleaved caspase-3-positive cells, suggesting that the transplanted cells have an anti-apoptotic function.

Expression of neurotrophic factors

The expression of several neurotrophic factors *VEGF*, *GDNF*, *NGF*, and *BDNF* was detected with *in situ* hybridization in the DiI-labeled CD31$^-$/CD146$^-$ SP cells in the peri-infarct area on day 21 (Fig. 4A–D). Real-time RT-PCR analysis demonstrated that expression of *VEGF* mRNA by the transplanted CD31$^-$/CD146$^-$ SP cells in the ischemic region on day 21 was 1,000 times and 28 times higher than that of normal porcine brain and that of the transplanted CD31$^-$/CD146$^-$ SP cells into normal rat striatum, respectively (Fig. 4E, F). Immunohistochemistry of VEGF showed that the VEGF protein was highly expressed in the DiI-labeled CD31$^-$/CD146$^-$ SP cells in the peri-infarct area on day 3 (Fig. 4G) compared with that on day 21 (Fig. 4H).

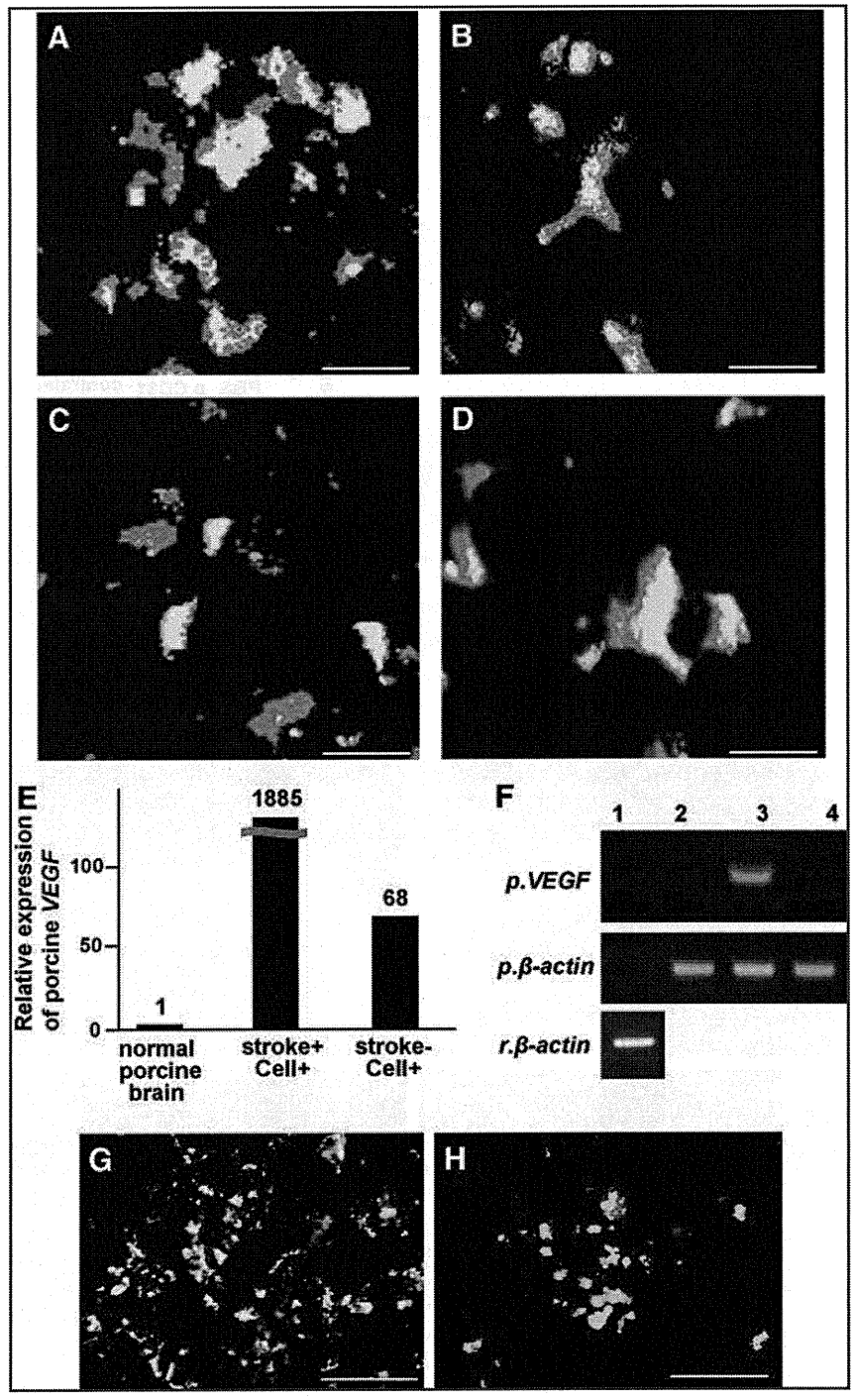

FIG. 4. Analysis of expression of *VEGF* **(A)**, *GDNF* **(B)**, *BDNF* **(C)**, and *NGF* **(D)** (green: **A–D)** of DiI-labeled transplanted CD31$^-$/CD146$^-$ SP cells (red) by *in situ* hybridization in the peri-infarct area. Real-time reverse transcription–polymerase chain reaction analysis of porcine *VEGF* (*pVEGF*) using porcine-specific primers **(E)**. Expression of porcine *VEGF* and porcine-specific and rat-specific β-actin 1, normal rat brain; 2, normal porcine brain; 3, peri-infarct area 21 days after transplantation of CD31$^-$/CD146$^-$ SP cells; 4, normal rat striatum 21 days after transplantation of the cells **(F)**. VEGF-positive cells on day 3 **(G)** and on day 21 **(H)** by immunohistochemistry. Scale bars = 10 μm **(A–D)** and 100 μm **(G, H)**. BDNF, brain-derived neurotrophic factor; GDNF, glial cell line-derived neurotrophic factor; NGF, nerve growth factor; VEGF, vascular endothelial growth factor. Color images available online at www.liebertonline.com/tea

Migration, proliferation, and anti-apoptotic assays

CM of CD31$^-$/CD146$^-$ SP cells showed higher migratory effect on SHSY5Y cells than VEGF, NGF, and BDNF, and was similar to GDNF (Fig. 5A). Its proliferation effect was higher than VEGF and NGF, and similar to BDNF and GDNF (Fig. 5B). Its anti-apoptotic activity was higher than BDNF, GDNF, and VEGF (Fig. 5C).

Evaluation of motor function

All groups (CD31$^-$/CD146$^-$ SP cells, unfractionated pulp cells, and PBS) displayed high score for motor function at the early stage (day 0, scores are 8.08±0.79; 8.25±0.96; 8.42±0.79, and day 2, 5.08±0.90; 6.25±1.26; 7.67±0.78, respectively). Progressive improvement in motor disability in the CD31$^-$/CD146$^-$ SP cell transplantation group after day 2 became significant on day 6 compared with PBS control group (2.67±1.23; 6.83±0.72), and more significant on day 9 compared with the unfractionated pulp cells and the PBS control group (1.33±0.78; 2.8±0.96; 6.50±0.67) (Fig. 6A). Persistent improvement in CD31$^-$/CD146$^-$ SP cells transplantation group was noted on day 14 (1.00±0.71) and 21 (0.80±0.45), whereas persistent impairment of motor disability (score above 4) was observed in the PBS group on day 14 (5.60±0.55) and 21 (5.40±0.59) (Fig. 6A). Further, the video image demonstrated significant recovery in motor function of the CD31$^-$/CD146$^-$ SP cell transplantation group compared with the unfractionated pulp cells and PBS control groups on day 6 (Supplementary Videos S1–S3; Supplementary Data are available online at www.liebertonline.com/tea).

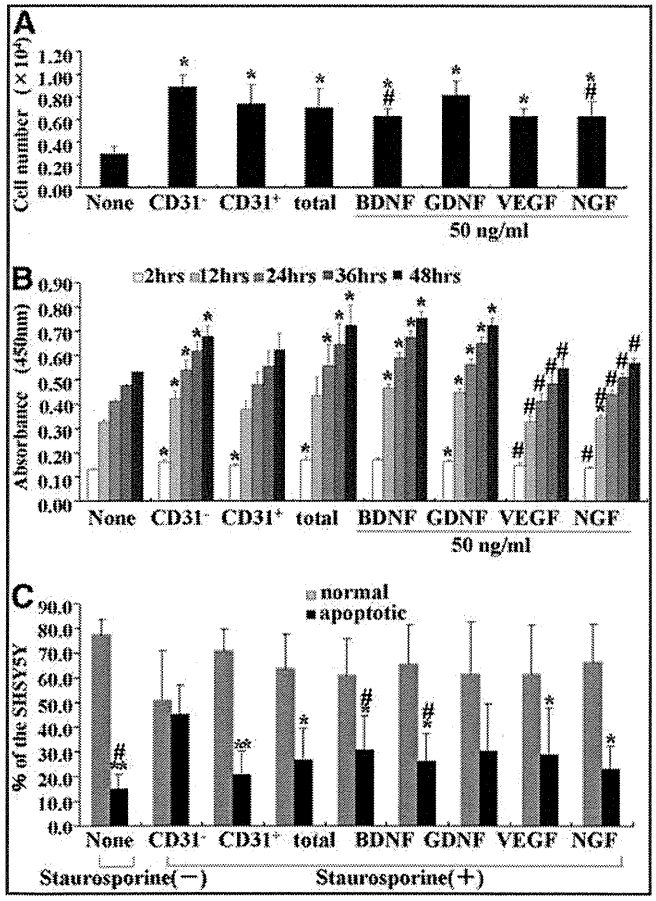

FIG. 5. The migration **(A)**, proliferative effect **(B)**, and anti-apoptotic effect **(C)** of conditioned medium of CD31$^-$/CD146$^-$ SP cells, CD31$^+$/CD146$^-$ SP cells, and unfractionated total pulp cells and neurotrophic factors on SHSY5Y cells. $^*p<0.05$, $^{**}p<0.005$, versus control. $^{\#}p<0.05$, versus CD31$^-$/CD146$^-$ SP cells. Data were expressed as means±SD at three determinations **(A, C)** and four determinations **(B)**. Student's *t*-test.

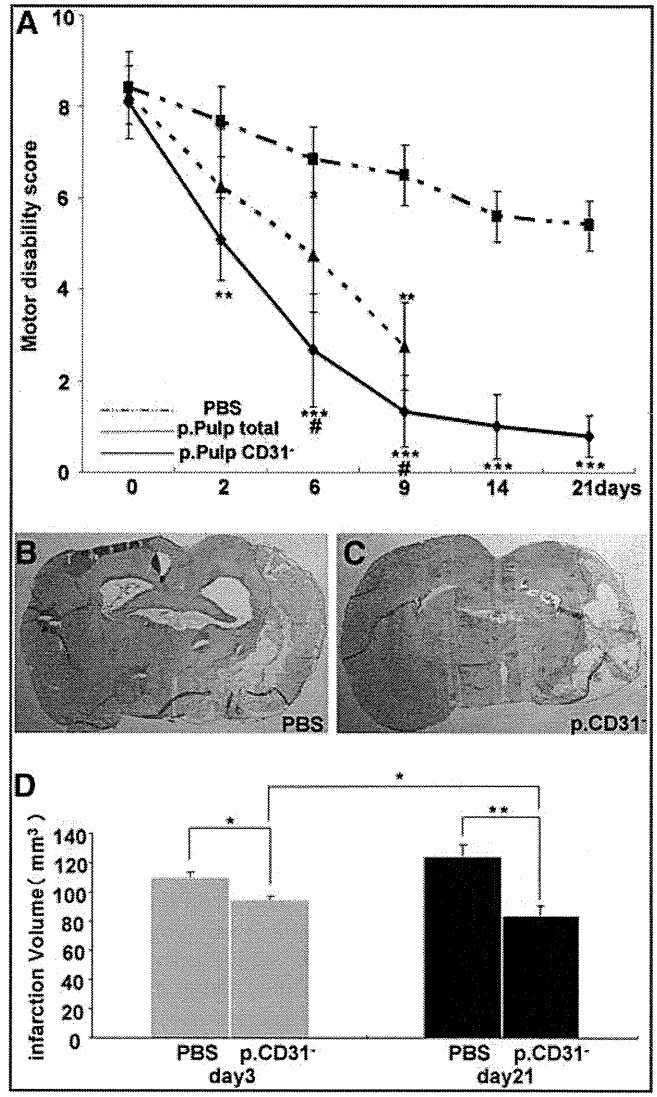

FIG. 6. Motor disability test by injection of the CD31$^-$/CD146$^-$ SP cells, the unfractionated pulp cells and the PBS on days 0, 2, 6, and 9 **(A)**. Infarct area on day 21 **(B, C)**. The reduction of the infarct volume 3 and 21 days after injection of CD31$^-$/CD146$^-$ SP cells **(D)**. $^*p<0.05$, $^{**}p<0.005$, $^{***}p<0.001$, versus control. $^{\#}p<0.05$, versus CD31$^-$/CD146$^-$ SP cells. Data were expressed as means±SD at three determinations **(D)**, Student's *t*-test.

Reduction of infarct volume

There was a significant decrease in the infarct volume on days 3 and 21 in the CD31$^-$/CD146$^-$ SP cell transplantation

group (day 3, 95.2±2.5 mm^3, n=3: day 21, 84.7±6.5 mm^3, n=4) compared to PBS group (day 3, 109.7±4.1 mm^3, n=3: day 21, 123.9±7.4 mm^3, n=4). The difference of infarct volume between the CD31$^-$/CD146$^-$ SP cell transplantation group and the PBS group increased over time (reduced by 13.3% on day 3 and reduced by 32.9% on day 21) (Fig. 6D). These results suggest that transplanted CD31$^-$/CD146$^-$ SP cells promoted the regeneration.

Discussion

In the current study, we demonstrated that transplanted CD31$^-$/CD146$^-$ SP cells migrated to the peri-infarct area. In addition, these cells released neurotrophic factors, and promoted migration and differentiation of the endogenous NPCs in SVZ. They also induced vasculogenesis in the peri-infarct area. These results indicate that CD31$^-$/CD146$^-$ SP cells ameliorated the ischemic tissue injury and accelerated the functional recovery after TMCAO. We have hypothesized that three mechanisms may contribute to the actions of VEGF. First, VEGF produced by transplanted cells may promote neurogenesis. NPCs in SVZ are known to migrate to the peri-infarct area and differentiate into neurons.[1] In this study, VEGF induced a chemotactic response in SHSY5Y cells. The transplanted CD31$^-$/CD146$^-$ SP cells migrated to the peri-infarct area and expressed VEGF. These results suggest that VEGF released by CD31$^-$/CD146$^-$ SP cells in the peri-infarct may promote migration of the endogenous NPCs in SVZ. Second, VEGF produced by transplanted cells may promote vasculogenesis. VEGF binds to its receptors on locally present vascular endothelial cells and directly initiates the angiogenic response.[12] In this study, the number of RECA1-positive endothelial cells significantly increased in the cell transplantation group. Third, VEGF may provide a neuroprotective effect. The neuroprotective effects of VEGF in experimental cerebral ischemia have been reported.[13] In cell the transplantation group, the number of cleaved caspase-3-immunopositive cells in the peri-infarct area was decreased compared with that in the PBS group, thus demonstrating the anti-apoptotic effects of VEGF on SHSY5Y cells. These results suggest that VEGF produced by CD31$^-$/CD146$^-$ SP cells may inhibit apoptosis of neurons. Thus, VEGF demonstrates pleiotropic effects on neurogenesis, vasculogenesis, and neuroprotection.

As VEGF is a potent vascular permeability factor, it may accelerate brain edema after stroke. Administration of VEGF in early ischemia (1 h after ischemia) leads to significant increase in blood–brain barrier leakage as well as enlarged ischemic areas.[14] However, VEGF administration at 24 h after TMCAO reduces infarct size, improves neurologic recovery, enhances neurogenesis in the SVZ and angiogenesis in the ischemic border zone.[14] In this study, CD31$^-$/CD146$^-$ SP cells were transplanted 24 h after TMCAO and we monitored the reduction of infarct size and improvement of motor disability. The time of administration of cells is critical. Thus, if CD31$^-$/CD146$^-$ SP cells were transplanted during an optimal window of time, they exhibit beneficial effects without the deleterious effects of edema.

In addition, CD31$^-$/CD146$^-$ SP cells expressed other neurotrophic factors such as GDNF,[15] NGF,[16] and *BDNF*[16] in the peri-infarct area. These neurotrophic factors had migratory, proliferative, and/or anti-apoptotic effects on SHSY5Y cells *in vitro* and may also contribute to the recovery from ischemic brain injury.

Finally, we explored the plausible underlying mechanisms of how injection of CD31$^-$/CD146$^-$ SP cells into the brains of immunocompetent rats staved off graft rejection. Blood–brain barrier is known to play a critical role in maintaining the immune-privileged status of the central nervous system.[17] It is well known that mesenchymal stem cells from bone marrow are not rejected by hosts and immunosuppression is not required in rodents.[1] Dental pulp stem cells have many similarities to mesenchymal stem cells; transplanted CD31$^-$/CD146$^-$ SP cells possess immunosuppressive properties.[18]

Conclusion

In summary, the transplantation of porcine CD31$^-$/CD146$^-$ SP cells promotes neurogenesis and vasculogenesis in an induced peri-infarct area, and enhances recovery after TMCAO in rats. Further research is needed to understand the underlying mechanisms. For potential clinical application and translational studies, the safety of CD31$^-$/CD146$^-$ SP cells must be assessed, including tumor formation. In conclusion, regeneration therapy using CD31$^-$/CD146$^-$ SP cells is a potential candidate in the treatment of stroke.

Acknowledgments

The authors thank Drs. Masataka Ito, Kayo Adachi, and Kiyomi Imabayasghi for their assistance. This work was supported by funds from Collaborative Development of Innovative Seeds, Potentiality verification stage from Japan Science and Technology Agency, a Grant-in-Aid for Scientific Research from the Ministry of Education, Science, Sports and Culture, Japan, No. 19659499 (M.N.), No. 20390504 (M.N.), and No. 18592173 (H.H.), and the Research Grant for Longevity Sciences (19C-2, 21A-7) from the Ministry of Health, Labour, and Welfare (M.N.).

Disclosure Statement

No competing financial interests exist.

References

1. Burns, T.C., Verfaillie C.M., and Low W.C. Stem cells for ischemic brain injury: a critical review. J Comp Neurol **515,** 125, 2009.
2. Locatelli, F., Bersano, A., Ballabio, E., Lanfranconi, S., Papadimitriou, D., Strazzer, S., Bresolin, N., Comi, G.P., and Corti, S. Stem cell therapy in stroke. Cell Mol Life Sci **66,** 757, 2009.
3. Gage, F.H., Kempermann, G., Palmer, T.D., Peterson, D.A., and Ray, J. Multipotent progenitor cells in the adult dentate gyrus. J Neurobiol **36,** 249, 1998.
4. Yang, K.L., Chen, M.F., Liao, C.H., Pang, C.Y., and Lin, P.Y. A simple and efficient method for generating Nurr1-positive neuronal stem cells from human wisdom teeth (tNSC) and the potential of tNSC for stroke therapy. Cytotherapy **11,** 606, 2009.
5. Iohara, K., Zheng, L., Wake, H., Ito, M., Nabekura, J., Wakita, H., Nakamura, H., Into, T., Matsushita, K., and Nakashima, M. A novel stem cell source for vasculogenesis in ischemia: subfraction of side population cells from dental pulp. Stem Cells **26,** 2408, 2008.

6. Longa, E.Z., Weinstein, P.R., Carlson, S., and Cummins, R. Reversible middle cerebral artery occlusion without craniectomy in rats. Stroke **20,** 84, 1989.
7. Koning, G., Colin, L., and Beyreuther, K. Retionic acid induced differentiated neuroblastoma cells show increased expression of the βA4 amyloid gene of Alzheimer's disease and an altered splicing pattern. FEBS Lett **269,** 305, 1990.
8. Richard, B., Eric, S., Patrick, O., Kurt, W., and Ywes, P. Induction of a common pathway of apoptosis by staurosporine. Exp Cell Res **211,** 314, 1994.
9. Leker, R.R., Gai, N., Mechoulam, R., and Ovadia, H. Drug-induced hypothermia reduces ischemic damage: effects of the cannabinoid HU-210. Stroke **34,** 2000, 2003.
10. Ginsberg, M.D. Adventures in the pathophysiology of brain ischemia: penumbra, gene expression, neuroprotection: the 2002 Thomas Willis Lecture. Stroke **34,** 214, 2003.
11. Leach, M.J., Swan, J.H., Eisenthal, D., Dopson, M., and Nobbs, M. BW619C89, a glutamate release inhibitor, protects against focal cerebral ischemic damage. Stroke **24,** 1063, 1993.
12. Plate, K.H., Beck, H., Danner, S., Allegrini, P.R., and Wiessner, C. Cell type specific upregulation of vascular endothelial growth factor in an MCA-occlusion model of cerebral infarct. J Neuropathol Exp Neurol **58,** 654, 1999.
13. Jin, K.L., Mao, X.O., and Greenberg, D.A. Vascular endothelial growth factor: direct neuroprotective effect in *in vitro* ischemia. Proc Natl Acad Sci U S A **97,** 10242, 2000.
14. Heike, B., and Karl, H.P. Angiogenesis after cerebral ischemia. Acta Neuropathol **117,** 481, 2009.
15. Leu-Fen, H., Lin, H., Doherty, D., Lile, B., and Frank, C. GDNF: a glial cell line-derived neurotrophic factor for midbrain dopaminergic neurons. Science **260,** 1072, 1993.
16. Shawne, N., Fernando, G., James, C., and Carl, C. Physical activity increases mRNA for brain-derived neurotrophic factor and nerve growth factor in rat brain. Brain Res **726,** 49, 1996.
17. Pachter, J.S., De Vries, H.E., and Fabry, Z. The blood-brain barrier and its role in immune privilege in the central nervous system. J Neuropathol Exp Neurol **62,** 593, 2003.
18. Pierdomenico, L., Bonsi, L., Calvitti, M., Rondelli, D., Arpinati, M., Chirumbolo, G., Becchetti, E., Marchionni, C., Alviano, F., Fossati, V., Staffolani, N., Franchina, M., Grossi, A., and Bagnara, G.P. Multipotent mesenchymal stem cells with immunosuppressive activity can be easily isolated from dental pulp. Transplantation **80,** 836, 2005.

Address correspondence to:
Misako Nakashima, Ph.D.
Department of Oral Disease Research
National Center for Geriatrics and Gerontology
Research Institute
35 Gengo, Morioka, Obu
Aichi 474-8522
Japan

E-mail: misako@ncgg.go.jp

Received: May 24, 2010
Accepted: January 10, 2011
Online Publication Date: February 22, 2011

THE JOURNAL OF BIOLOGICAL CHEMISTRY VOL. 286, NO. 11, pp. 8952–8960, March 18, 2011

Plasminogen/Plasmin Modulates Bone Metabolism by Regulating the Osteoblast and Osteoclast Function*

Received for publication, June 7, 2010, and in revised form, January 4, 2011 Published, JBC Papers in Press, January 14, 2011, DOI 10.1074/jbc.M110.152181

Yosuke Kanno[‡1], Akira Ishisaki[§], Eri Kawashita[‡], Naoyuki Chosa[§], Keiichi Nakajima[¶], Tatsuji Nishihara[‖], Kuniaki Toyoshima[**], Kiyotaka Okada[‡‡], Shigeru Ueshima[‡‡§§], Kenji Matsushita[¶¶], Osamu Matsuo[‡‡], and Hiroyuki Matsuno[‡]

From the [‡]Department of Clinical Pathological Biochemistry, Faculty of Pharmaceutical Science, Doshisha Women's Collage of Liberal Arts, 97-1 Kodo Kyo-tanabe, Kyoto 610-0395, the [§]Department of Biochemistry, Iwate Medical University School of Dentistry, 1-3-27, Chuo-dori, Morioka, Iwate 020-8505, the [¶]Department of Animal Production and Grassland, National Agricultural Research Center for Hokkaido Region, 062-8555 Sapporo, the [‖]Division of Infections and Molecular Biology, Department of Health Promotion, Kyushu Dental College, 2-6-1 Manazuru, Kokurakita-ku, Kitakyushu 803-8580, the [**]Division of Oral Histology and Neurobiology, Department of Biosciences, Kyushu Dental College, 2-6-1 Manazuru, Kokurakita-ku, Kitakyushu 803-8580, the [‡‡]Department of Physiology II, Kinki University School of Medicine 377-2 Ohnohigashi, Osaka-sayama-city 589-8511, the [§§]Department of Food Science and Nutrition, Kinki University School of Agriculture, Nara 631-8505, and the [¶¶]Laboratory of Oral Disease Research, National Institute for Longevity Sciences, National Center for Geriatrics and Gerontology, 36-3 Gengo, Morioka, Obu, Aichi 474-8522, Japan

The contribution of plasminogen (Plg)/plasmin, which have claimed to be the main fibrinolytic regulators in the bone metabolism, remains unclear. This study evaluated how the absence of Plg affects the function of osteoblast (OB) and osteoclast (OC). There was a larger population of pre-OCs in bone marrow-derived cells from the $Plg^{-/-}$ mice than the population of that from the WT mice. In addition, the absence of Plg suppressed the expression of osteoprotegerin in OBs. Moreover, an exogenous plasmin clearly induced the osteoprotegerin expression in $Plg^{-/-}$ OBs. The osteoclastogenesis of RAW264.7 mouse monocyte/macrophage lineage cells in co-culture with OBs from the $Plg^{-/-}$ mice was significantly accelerated in comparison with that in co-culture with OBs from the WT mice. Intriguingly, the accelerated OC differentiation of RAW264.7 cells co-cultured with $Plg^{-/-}$ OBs was clearly suppressed by the treatment of an exogenous plasmin. Consequently, $Plg^{-/-}$ mice display decreased bone mineral density. These findings could eventually lead to the development of new clinical therapies for bone disease caused by a disorder of the fibrinolytic system.

The fibrinolytic system contains plasminogen (Plg),[2] a proenzyme, which is converted to the active serine protease plasmin, a main component of the fibrinolytic system, through the action of a tissue-type plasminogen activator (tPA) or urokinase-type PA (uPA). The inhibition of the system may occur through the neutralization of the plasminogen activators or plasmin, and this neutralization is achieved mainly by the plasminogen activator inhibitor-1 (PAI-1) or α2-antiplasmin (α2AP), respectively. PAI-1, the primary endogenous inhibitor of tPA or uPA, plays an important role in inhibiting arterial clot lysis (1). α2AP rapidly inactivates plasmin, resulting in the formation of a stable inactive complex, plasmin-α2AP (2). Apart from the removal of fibrin, the fibrinolytic system also plays a pivotal role in such phenomena as embryogenesis, proliferation, migration, wound healing, fibrosis, and tumorigenesis (3–9).

It is suggested that fibrinolytic factors such as tPA, uPA, uPA receptor, and PAI-1 are involved in bone metabolism as follows. The absence of tPA and uPA enhanced OB differentiation and formation of a mineralized bone matrix and increased bone formation and bone mass (10). The absence of PAI-1 protects against trabecular bone loss induced by estrogen deficiency, suggesting a site-specific role for PAI-1 in bone turnover (11). In addition, uPA receptor-lacking mice displayed increased bone mineral density (BMD), increased osteogenic potential of OBs, decreased OC formation, and cytoskeletal reorganization in mature OCs (12). However, the physiological roles of fibrinolytic main regulators such as Plg/plasmin in bone metabolism are not precisely understood.

The receptor activator of NF-κB (RANK), its ligand RANKL, and OPG control OC function (13, 14). RANK activated by RANKL has proven to be absolutely required for OC development (15). RANKL is neutralized by OPG that specifically binds to RANKL. OPG is expressed in many tissues apart from OBs, including heart, kidney, liver, spleen, and bone marrow (13). However, molecular mechanisms of OPG expression remain to be elucidated. We herein report the crucial role of fibrinolytic main regulators Plg/plasmin in bone metabolism especially on the point of view of how the regulators affect the ability of pre-OCs in bone marrow to differentiate into OCs, OBs to induce OC differentiation, and OBs to mineralize extracellular matrix.

* This work was supported by Grant-in-aid for Young Scientists B:21790097 (to Y. K.) from the Ministry of Education, Culture, Sports, Science and Technology, Japan Society for the Promotion of Science, and Grant-in-aid for Strategic Medical Science Research Center from the Ministry of Education, Culture, Sports, Science and Technology of Japan, 2010-2014.

[1] To whom correspondence should be addressed. Tel.: 81-0774-65-8629; Fax: 81-0774-65-8479; E-mail: ykanno@dwc.doshisha.ac.jp.

[2] The abbreviations used are: Plg, plasminogen; TRAP, tartrate-resistant acid phosphatase; OC, osteoclast; OB, osteoblast; OPG, osteoprotegerin; BMD, bone mineral density; PGE_2, prostaglandin E_2; RANK, receptor activator of NF-κB; RANKL, RANK ligand; tPA, tissue-type plasminogen activator; uPA, urokinase-type PA; PAI-1, plasminogen activator inhibitor-1; M-CSF, macrophage colony-stimulating factor; ALP, alkaline phosphatase; qRT, quantitative RT.

MATERIALS AND METHODS

All experiments were performed in accordance with the Guide for the Care and Use of Laboratory Animals published by the National Institutes of Health.

Animals—The Plg-deficient ($Plg^{-/-}$) mice (16) were kindly provided by Prof. D. Collen (University of Leuven, Belgium).

Wild type (WT) and $Plg^{-/-}$ mice littermates were housed in groups of two to five in filter-top cages with a fixed 12-h light, 12-h dark cycle. The body weights of mice were measured weekly.

Reagents—Plasmin, aprotinin, α2AP, ϵ-aminocaproic acid, and other chemical substances were obtained from Sigma.

Cell Culture—Bone marrow cells, RAW264.7 mouse monocyte/macrophage lineage cells (American Type Culture Collection), and primary OBs were maintained in α-minimal essential medium (Invitrogen) supplemented with 10% fetal bovine serum (FBS) (Hyclone, Logan, UT) and 1% penicillin/streptomycin (Invitrogen) at 37 °C in a humidified atmosphere of 5% CO_2, 95% air. Primary OBs derived from mice calvaria were obtained as described previously (17).

OC Differentiation Assay—Bone marrow-derived cells that include a population of pre-OCs were obtained from tibia of 5–7-week-old adult mice. Mouse bone marrow cells were cultured for 3 days with RANKL (100 ng/ml) and M-CSF (100 ng/ml) in 48-well plates. In other experiments, RAW264.7 cells were co-cultured with OBs from the $Plg^{+/+}$ and $Plg^{-/-}$ mice for 3 days in the absence or presence of interleukin-1β (IL-1β) (5 ng/ml) or prostaglandin E_2 (PGE_2) (1 μM) in 48-well plates. Cells were then fixed and stained for tartrate-resistant acid phosphatase (TRAP; a marker enzyme of OCs) as described previously (17). TRAP-positive multinucleated cells containing three or more nuclei were counted as OCs, under microscopic examination.

Bone Resorption Assay—To estimate bone resorption activity of differentiated OCs from bone marrow cells of the $Plg^{+/+}$ and $Plg^{-/-}$ mice, the cells were stimulated with RANKL (100 ng/ml) and M-CSF (100 ng/ml) for 7 days on the BioCoat™ Osteologic™ multiple test slides, which consisted of submicron synthetic calcium phosphate thin film coated onto various culture vessels (BD Biosciences). The nonresorbed area of calcium phosphate film was then visualized by using a method of von Kossa staining, as follows. After fixation of the cells in the culture with 5% glutaraldehyde, the calcium phosphate film was treated with 5% silver nitrate for 30 min. Then the staining was developed with 5% sodium carbonate in 25% formalin. The stained film in each well was photographed under light microscopy, and then the image was inverted to yield the negative image; the black image represents the resorbed area in the calcium phosphate film.

Bone Histology—Bone histomorphometry of tibia in 5-week-old male $Plg^{+/+}$ and $Plg^{-/-}$ mice was performed. Each tibia was removed and fixed in 4% paraformaldehyde for 2 days and then demineralized with 10% EDTA for 14 days before embedding in paraffin. Paraffin-embedded tissue was serially sectioned at a distance of 4–7 μm. Then the sections were stained with hematoxylin and eosin (H&E) and TRAP by using a TRAP kit (Sigma). For the quantitative evaluation of the intensity of TRAP staining of bone marrow tissue in decalcified sections of tibia from the $Plg^{+/+}$ and $Plg^{-/-}$ mice, the TRAP-stained images obtained from separate fields on the specimens ($n = 6$) were analyzed by using ImageJ.

Measurement of Bone Mineral Density—BMD was measured as described by Kanazawa *et al.* (18) and Nishiwaki *et al.* (19). BMD of the proximal tibia of the $Plg^{+/+}$ and $Plg^{-/-}$ mice at the indicated time was evaluated by using peripheral quantitative computed tomography with a fixed x-ray fan beam of 50-μm spot size, at 1 mA and 50 kV (LaTheta LCT-100S; Aloka, Tokyo, Japan).

RNA Isolation and Quantitative RT-PCR—Total RNA was extracted as described previously (6). First strand cDNA was synthesized from total RNA by using the PrimeScript RT reagent kit (Takara). Quantitative RT-PCR (qRT-PCR) was performed on the IQ5 real time PCR detection system (Bio-Rad) with SYBR Green technology on cDNA generated from the reverse transcription of purified RNA. The two-step PCRs were performed at 92 °C for 1 s and 60 °C for 10 s. OPG mRNA expression was normalized against GAPDH mRNA expression using the comparative cycle threshold method. We used the following primer sequence: OPG, 5′-CAATGGCTGGCTTGGTTTCATAG-3′ and 5′-CTGAACCAGACATGACAGCTGGA-3′; GAPDH, 5′-TGTGTCCGTCGTGGATCTGA-3′ and 5′-TTGCTGTTGAAGTCGCAGGAG-3′.

Western Blot Analysis—We performed a Western blot analysis for detection of OPG, phospho-ERK1/2, phospho-p38 MAPK, ERK1/2, and p38 MAPK as described previously (20). We detected OPG, phospho-ERK1/2, phospho-p38 MAPK, ERK1/2, and p38 MAPK by incubation with a polyclonal OPG antibody (rabbit IgG, from GeneTex Inc.), anti-phospho-ERK1/2 antibody (Cell Signaling Technology, Danvers, MA), anti-phospho-p38 MAPK antibody (Cell Signaling Technology, Danvers, MA), anti-ERK1/2 antibody (Cell Signaling Technology, Danvers, MA), and anti-p38 MAPK antibody (Cell Signaling Technology, Danvers, MA).

Measurement of Alkaline Phosphatase Activity—We measured alkaline phosphatase (ALP) activity as described previously (20). Primarily cultured OBs were cultured for 14 day with differentiation media (media supplemented with 10 mM β-glycerophosphate and 10 nM dexamethasone and 50 μg/ml ascorbic acid) in 6-well plates. After 14 days, cells were then washed, and proteins in cells were extracted with a lysis buffer (10 mM Tris-HCl, pH 7.5, 0.1% Triton X-100). ALP activity was determined using *p*-nitrophenyl phosphate (Sigma) as a substrate.

Statistical Analysis—All data are expressed as mean ± S.E. The significance of the effect of each treatment ($p < 0.05$) was determined by analysis of variance followed by the Student's Newman-Keuls test.

RESULTS

Histological and Radiological Evaluation of the Status of Endochondral Ossification in Plg-deficient Mice—The BMDs in the $Plg^{+/+}$ and $Plg^{-/-}$ mice at 4–20 weeks were radiologically assessed using peripheral quantitative computed tomography. Intriguingly, the trabecular BMD in tibia from the $Plg^{-/-}$ mice was significantly lower than that from the $Plg^{+/+}$ mice at 4–6 weeks after birth (Fig. 1*A*). In addition, the cortical BMD in tibia

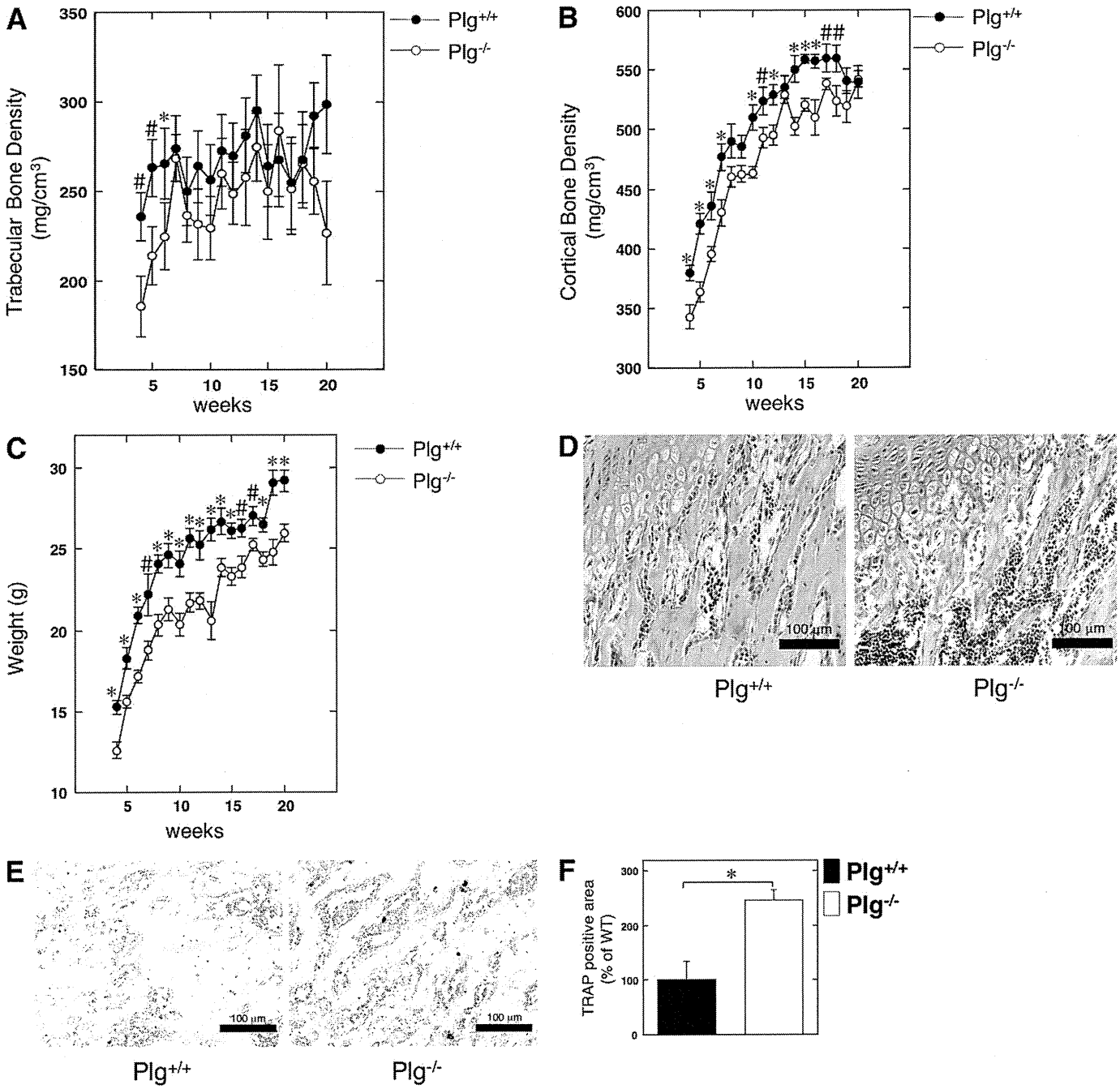

FIGURE 1. **Bone histomorphometry and bone mineral density in Plg-deficient mice.** *A*, trabecular BMD in the proximal tibia of male $Plg^{+/+}$ and $Plg^{-/-}$ mice was obtained from pQCT measurement ($n = 13$). *B*, cortical BMD in the proximal tibia of the $Plg^{+/+}$ and $Plg^{-/-}$ mice was obtained from pQCT measurement ($n = 13$). *C*, growth curves of the $Plg^{+/+}$ and $Plg^{-/-}$ mice ($n = 13$). *D* and *E*, bone histomorphometry of tibia in 5-week-old male $Plg^{+/+}$ and $Plg^{-/-}$ mice (*D*, H&E; *E*, TRAP). *D*, layer of chondrocytes and trabecular bone formation in the medullary cavities were observed in both $Plg^{+/+}$ and $Plg^{-/-}$ mice. *E*, TRAP-positive area in the bone marrow tissue of the tibias from $Plg^{-/-}$ mice was much larger than that in the tissue specimens obtained from $Plg^{+/+}$ mice. *F*, intensity of TRAP staining on the decalcified sections of bone marrow tissue in the $Plg^{+/+}$ and $Plg^{-/-}$ mice was quantitatively evaluated as described under "Materials and Methods" ($n = 6$). The intensity of TRAP staining on the sections from the $Plg^{-/-}$ mice was much stronger than that of sections from $Plg^{+/+}$ mice. The data represent the mean ± S.E. *, $p < 0.01$; #, $p < 0.05$.

from the $Plg^{-/-}$ mice was significantly lower than that from the $Plg^{+/+}$ mice at 4–18 weeks after birth (Fig. 1*B*). The decrease of cortical BMD seemed to parallel that of the body weight decrease in the $Plg^{-/-}$ mice at 4–18 weeks after birth (Fig. 1, *B* and *C*). Next, the status of endochondral ossification in tibia from the $Plg^{+/+}$ and $Plg^{-/-}$ was histologically compared to clarify the effect of the fibrinolytic system in bone metabolism. As shown in Fig. 1*D*, H&E staining of a decalcified section of tibia from the 5-week-old mice showed that the layer of chondrocytes and trabecular bone formation in the medullary cavities were observed in both $Plg^{+/+}$ and $Plg^{-/-}$ mice. The TRAP staining of the decalcified section of the tibias from the 5-week-old mice revealed that the area of TRAP-positive bone marrow tissue in the tibias from the $Plg^{-/-}$ mice was significantly larger than that of the tissue from the $Plg^{+/+}$ mice (Fig. 1*E*). In addition, the intensity of the TRAP staining on the decalcified sec-

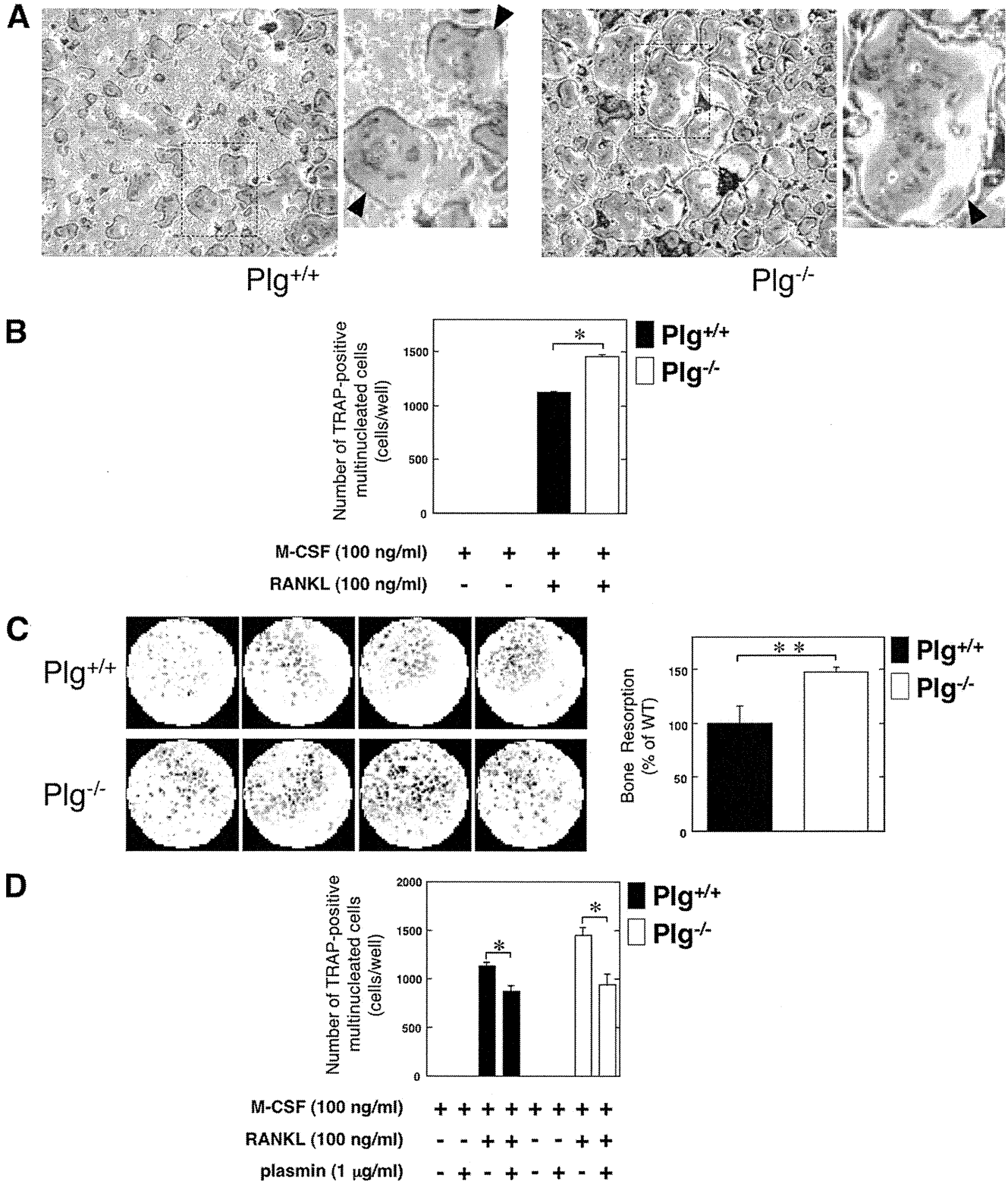

FIGURE 2. **Effect of Plg deficiency on osteoclastogenesis and the OC function.** *A*, bone marrow cells from the $Plg^{+/+}$ and $Plg^{-/-}$ mice were cultured for 3 days in the absence or presence of RANKL (100 ng/ml) and M-CSF (100 ng/ml). Mature OCs were identified as TRAP-positive multinucleated cells. The magnified image of *boxed area* was showed on the *right* of the original image. The *arrowheads* indicate osteoclasts. *B*, number of TRAP-positive multinucleated cells in *A* was determined from three different cultures. *C*, bone resorption activity of OCs differentiated from bone marrow-derived cells obtained from the $Plg^{+/+}$ and $Plg^{-/-}$ mice was compared. Bone marrow-derived cells from the $Plg^{+/+}$ and $Plg^{-/-}$ mice were cultured on the BioCoat™ Osteologic™ multiple test slides, which consisted of submicron synthetic calcium phosphate thin film coated onto various culture vessels, for 7 days in the presence of RANKL (100 ng/ml) and M-CSF (100 ng/ml) ($n = 4$). Next, the resorbed areas of the calcium phosphate film were visualized as described under "Materials and Methods." The *histogram, right panel*, shows quantitative representations of bone resorption obtained from densitometry analysis. The densitometry results were expressed as the mean density. *D*, bone marrow cells from the $Plg^{+/+}$ and $Plg^{-/-}$ mice were cultured for 3 days in the presence of M-CSF (100 ng/ml). Some cells were cultured in the presence or absence of RANKL (100 ng/ml) or plasmin (1 μg/ml) as indicated. The number of multinucleated TRAP-positive cells was determined from four different cultures. The data represent the mean ± S.E. *, $p < 0.01$; **, $p < 0.05$.

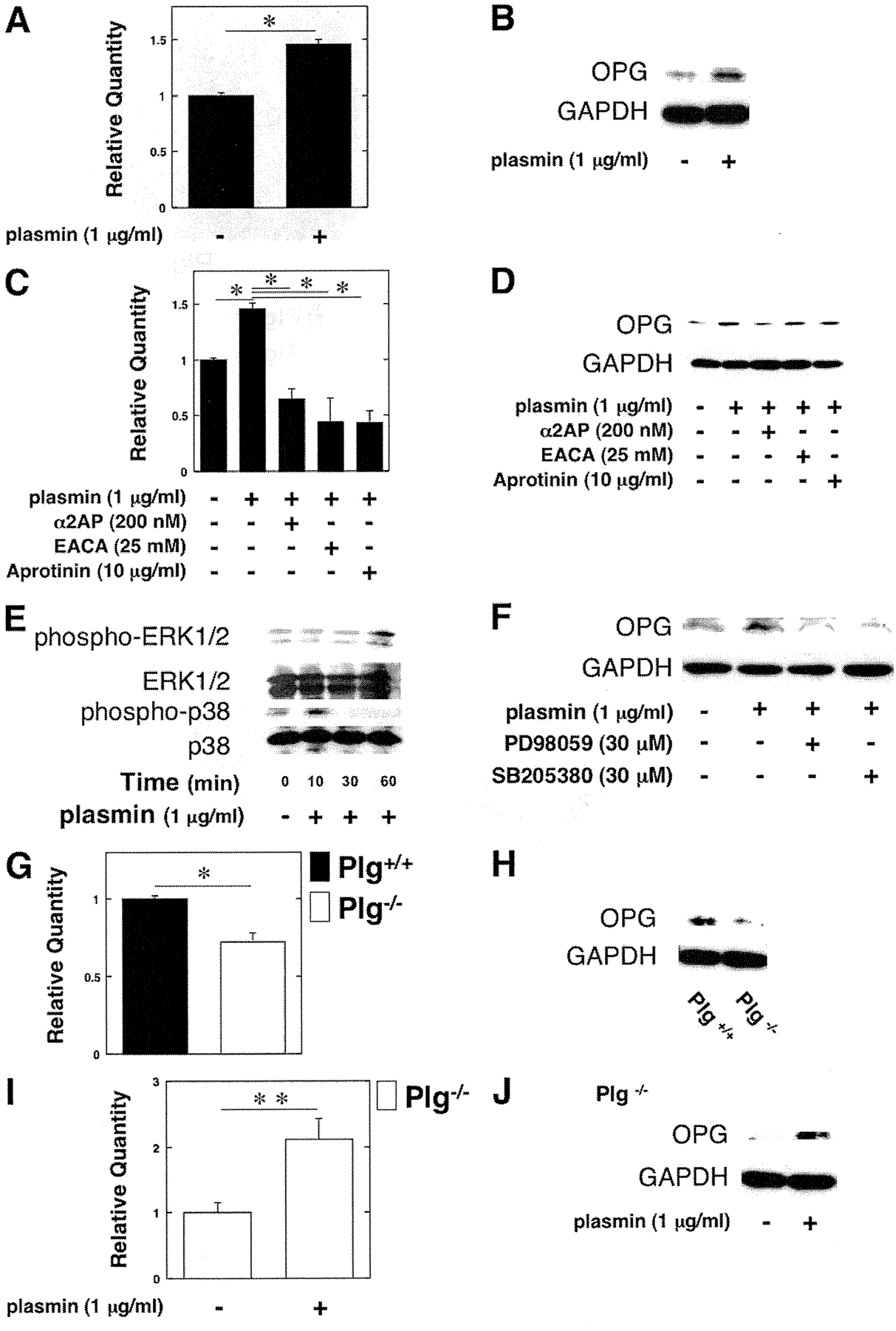

tions of bone marrow tissue in the $Plg^{+/+}$ and $Plg^{-/-}$ mice was quantitatively evaluated as described under "Materials and Methods." As shown in Fig. 1*F*, the intensity of TRAP staining on decalcified sections of bone marrow tissue in tibias from the $Plg^{-/-}$ mice was much stronger than in those from the $Plg^{+/+}$ mice.

Effect of the Plg Deficiency on the Osteoclastogenesis of Bone Marrow-derived Cells—We evaluated how the fibronolytic system affects OC differentiation and function. The pre-OC population in bone marrow-derived cells from the $Plg^{+/+}$ and $Plg^{-/-}$ mice were evaluated after stimulation with RANKL and M-CSF, respectively. As shown in Fig. 2*A*, many TRAP-positive multinucleated OCs were observed in bone marrow cell cultures derived from the $Plg^{-/-}$ mice tibia. Therefore, an up-regulation of the TRAP-positive cell number in the $Plg^{-/-}$ mice-derived bone marrow cells was observed (Fig. 2*B*). In addition, the bone resorption activity of OCs differentiated from bone marrow-derived cells was compared in the $Plg^{+/+}$ and $Plg^{-/-}$ mice. There was an up-regulation of the bone resorption activity of $Plg^{-/-}$ mice-derived bone marrow cells (Fig. 2*C*). Intriguingly, plasmin significantly inhibited the M-CSF- and RANKL-induced OC differentiation of bone marrow cells derived from the $Plg^{-/-}$ and $Plg^{+/+}$ mice (Fig. 2*D*).

Plasmin Induced the OPG Expression in OBs—To clarify how plasmin suppresses osteoclastogenesis *in vivo*, we examined whether plasmin up-regulates the expression of OPG in OBs from the WT mice *in vitro* by qRT-PCR and a Western blot analysis. Plasmin clearly induced OPG expression in OBs from the WT mice (Fig. 3, *A* and *B*). In addition, the effect of various plasmin inhibitors (α2AP; serine protease inhibitor, aprotinin; lysine analog, ϵ-aminocaproic acid) on plasmin-induced OPG expression was investigated. These plasmin inhibitors clearly abrogated the plasmin-induced OPG expression (Fig. 3, *C* and *D*).

In addition, we examined the plasmin-stimulated phosphorylation of ERK1/2 and p38 MAPK to determine whether plasmin activates ERK1/2 and p38 MAPK in OBs. Plasmin activated ERK1/2 and p38 MAPK in OBs (Fig. 3*E*). We also examined whether the ERK1/2 and p38 MAPK pathways are associated with the plasmin-induced expression of OPG in OBs by using the inhibitor of MEK and p38 MAPK (PD98059 and SB203580). PD98059 and SB203580 attenuated plasmin-induced expression of OPG in OBs (Fig. 3*F*). These data suggest that plasmin induces OPG expression through the ERK1/2 and p38 MAPK pathways.

Moreover, qRT-PCR and a Western blot analysis revealed that the expression of OPG was suppressed in OBs from the $Plg^{-/-}$ mice (Fig. 3, *G* and *H*), thus suggesting that the absence of plasmin may result in the acceleration of osteoclastogenesis of pre-OCs in accordance with the depletion of OPG synthesis in OBs. There was no difference in the status of RANKL mRNA expression in OBs from the $Plg^{+/+}$ and $Plg^{-/-}$ mice (data not shown). Moreover, plasmin induced OPG expression in $Plg^{-/-}$ OBs (Fig. 3, *I* and *J*).

Effects of Plg Deficiency on the Ability of OBs to Induce Osteoclastogenesis of RAW264.7 Mouse Monocyte/Macrophage Lineage Cells—The status of OC differentiation of RAW264.7 mouse monocyte/macrophage lineage cells in co-culture with $Plg^{-/-}$ OBs was examined to clarify how Plg deficiency affects OB function for osteoclastogenesis. The ability of $Plg^{-/-}$ OBs to induce OC differentiation of pre-OC RAW264.7 cells was compared with $Plg^{+/+}$ OBs. The OBs were co-cultured with RAW264.7 cells under stimulation with the inflammatory mediators interleukin 1-β (IL-1β) or prostaglandin E_2 (PGE_2). Inflammatory mediators induce RANKL expression on OBs (21). The inflammatory mediator-induced RANKL expression on OBs was expected to induce the osteoclastogenesis of the co-cultured RAW264.7 cells. As shown in Fig. 4*A*, IL-1β or PGE_2 increased the number of TRAP-positive multinucleated cells co-cultured with OBs. Intriguingly, the number of TRAP-positive multinucleated cells co-cultured with $Plg^{-/-}$ OBs lacking OPG expression was significantly higher than that co-cultured with $Plg^{+/+}$ OBs with or without IL-1β or PGE_2. In addition, the number of TRAP-positive multinucleated cells co-cultured with $Plg^{-/-}$ OBs was decreased by plasmin (Fig. 4*B*).

Effect of Plg Deficiency on the ALP Activity in OBs—The ALP activity in $Plg^{-/-}$ OBs was compared with $Plg^{+/+}$ OBs under stimulation with OB differentiation media as described under "Materials and Methods." The absence of Plg did not affect the ALP activity in undifferentiated and differentiated OBs (Fig. 5).

Rescue of the Down-regulated BMD in Plg-deficient Mice by the Injection of Plasmin—To clarify the effect of exogenous plasmin on bone formation *in vivo*, we evaluated the status of the BMD in the $Plg^{-/-}$ mice with or without plasmin injection. The plasmin injection clearly increased the trabecular BMD in the $Plg^{-/-}$ mice (Fig. 6*A*). However, the plasmin injection did not affect the cortical BMD and the weight in the $Plg^{-/-}$ mice (Fig. 6, *B* and *C*).

DISCUSSION

Fibrinolytic factors have been suggested to play an important role in bone metabolism. PAs and PAI-1 are involved in bone resorption by OCs (22, 23). However, the role of Plg/plasmin in bone metabolism was not precisely understood. This study showed that Plg/plasmin plays an important role in bone metabolism by regulating the function of both OBs and OCs.

FIGURE 3. **Plasmin induced the OPG expression in OBs.** *A–D*, OBs from the WT mice were cultured for 24 h in either the absence or presence of plasmin (1 μg/ml). Plasmin-induced expression of OPG gene in OBs from the WT mice was evaluated by qRT-PCR (*A*) or a Western blot analysis (*B*). *C* and *D*, some cultures were further treated with plasmin inhibitors as follows: α2AP (200 nM), ϵ-aminocaproic acid (25 mM), and aprotinin (10 μg/ml). The expression of OPG mRNA in OBs from the WT mice was then measured by qRT-PCR (*C*) or a Western blot analysis (*D*). *E*, OBs from the WT mice were stimulated with 1 μg/ml plasmin for the indicated periods. Phosphorylation of ERK1/2 and p38 MAPK was evaluated by a Western blot analysis using antibodies to ERK1/2 and p38 MAPK. *F*, OBs from the WT mice were pretreated with 30 μM PD98059 or 30 μM SB203580 for 60 min and then stimulated with 1 μg/ml plasmin for 24 h. The expression of OPG in OBs from the WT mice was evaluated by a Western blot analysis. *G* and *H*, OPG expression in OBs from the $Plg^{+/+}$ and $Plg^{-/-}$ mice was evaluated by qRT-PCR (*G*) or a Western blot analysis (*H*). *I* and *J*, OBs from the $Plg^{-/-}$ mice were cultured for 24 h in the absence or presence of plasmin (1 μg/ml). The OPG expression in OBs from the $Plg^{-/-}$ mice was evaluated by qRT-PCR (*I*) or a Western blot analysis (*J*). The data represent the mean of three individual experiments ± S.E. *, $p < 0.01$; **, $p < 0.05$.

The trabecular BMD in the tibias from the $Plg^{-/-}$ mice was significantly lower than that from the $Plg^{+/+}$ mice at 4–6 weeks after birth (Fig. 1*A*). In contrast, the cortical BMD in the tibias from the $Plg^{-/-}$ mice was significantly lower than that from the $Plg^{+/+}$ mice at 4–18 weeks after birth (Fig. 1*B*). Therefore, the decrease in the trabecular BMD in $Plg^{-/-}$ mice seemed to be transient; however, the decrease in the cortical BMD in the mice was consistently observed from the juvenile growth period to adulthood. In addition, TRAP staining of decalcified sections of tibias from the 5-we-old mice revealed that the intensity of TRAP staining of bone marrow tissue in the tibias from the $Plg^{-/-}$ mice was significantly stronger than that from the $Plg^{+/+}$ mice (Fig. 1, *E* and *F*). Thus, the histoenzymatic assessment indicated that the OC differentiation in bone marrow tissue of the $Plg^{-/-}$ mice might be more vigorously induced than that in the $Plg^{+/+}$ mice.

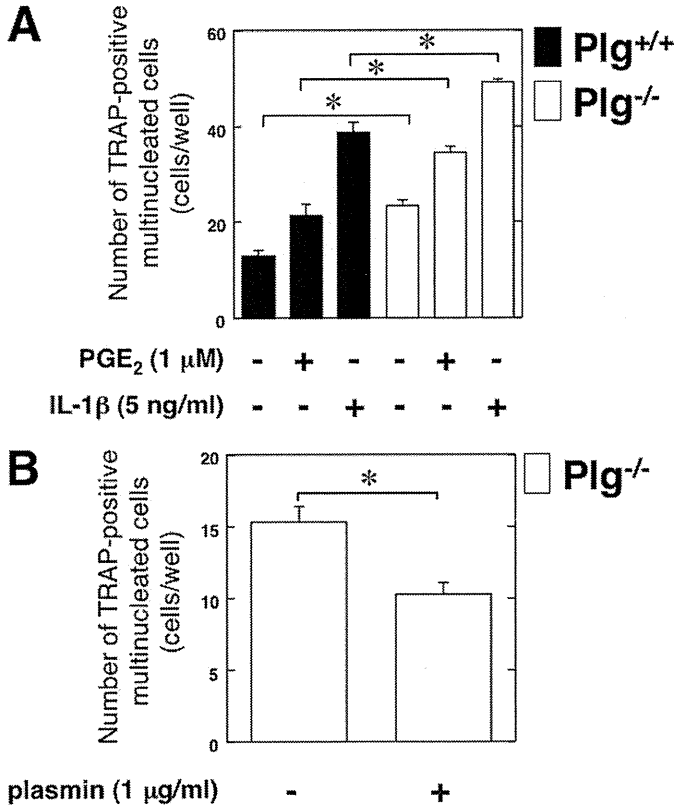

FIGURE 4. **Effects of Plg deficiency on the ability of OBs to induce osteoclastogenesis of RAW264.7 cells.** *A*, RAW264.7 cells and OBs from the $Plg^{+/+}$ and $Plg^{-/-}$ mice were co-cultured for 3 days in the absence or presence of IL-1β or PGE_2. *B*, RAW264.7 cells and OBs from the $Plg^{-/-}$ mice were co-cultured for 3 days in the absence or presence of plasmin. Mature OCs were identified as multinucleated TRAP-positive cells. The number of multinucleated TRAP-positive cells was determined from six different cultures. The data represent the mean ± S.E. *, $p < 0.01$.

The binding of RANKL to its receptor RANK triggers intricate and distinct signaling cascades that control lineage commitment and osteoclast activation (13). OPG inhibits osteoclast formation and bone resorption by blocking RANKL/RANK interactions (14). This study showed that plasmin increased the OPG expression in WT OBs (Fig. 3, *A–D*). Moreover, the expression level of OPG was decreased in $Plg^{-/-}$ OBs compared with $Plg^{+/+}$ OBs (Fig. 3, *G* and *H*), suggesting that absence of plasmin may result in an acceleration of OB-mediated osteoclastogenesis of pre-OCs in accordance with the depletion of OPG expression in OBs. In fact, the number of TRAP-positive multinucleated RAW264.7 cells co-cultured with $Plg^{-/-}$ OBs was significantly higher than that of the cells co-cultured with $Plg^{+/+}$ OBs (Fig. 4*A*). Intriguingly, plasmin significantly inhibited the M-CSF- and RANKL-induced OC differentiation of bone marrow cells derived from the $Plg^{+/+}$ and $Plg^{-/-}$ (Fig. 2*D*), suggesting that plasmin might attenuate osteoclastogenesis by its direct effects on pre-OCs. In addition, there was a larger population of pre-OCs in bone marrow-derived cells from the $Plg^{-/-}$ mice in comparison with the $Plg^{+/+}$ mice (Fig. 2, *A–C*). The level of ALP activity in $Plg^{-/-}$ OBs was similar to that in $Plg^{+/+}$ OBs (Fig. 5), thus suggesting that the bone-mineralizing activity of OBs in the $Plg^{-/-}$ mice might be comparable with that in the $Plg^{+/+}$ mice. Consequently, the $Plg^{-/-}$ mice display decreased bone mineral density in accordance with the enhanced ability of OBs to induce osteoclastogenesis of pre-OCs, the loss of the direct and suppressive effect of plasmin on pre-OCs differentiating into mature OCs, and the increased pre-OC population in bone marrow cells. In fact, the injection of plasmin into the $Plg^{-/-}$ mice clearly rescued the diminished trabecular BMD during the juvenile growth period (Fig. 6).

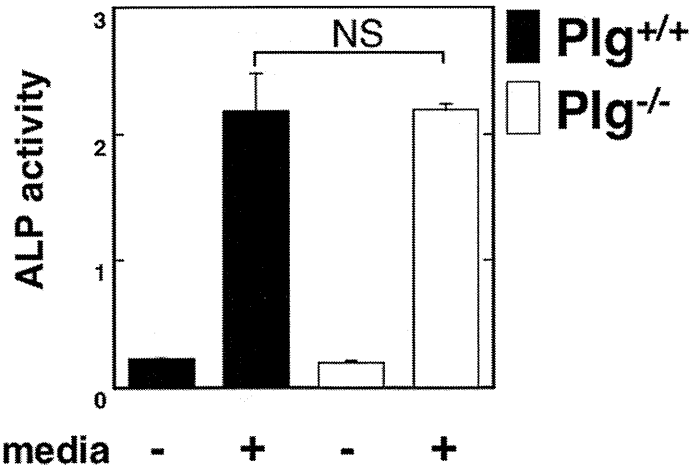

FIGURE 5. **Effect of Plg deficiency on the ALP activity in OBs.** ALP activity in OBs from the $Plg^{+/+}$ and $Plg^{-/-}$ mice was evaluated ($n = 4$). The data represent the mean ± S.E. *NS*, not significant.

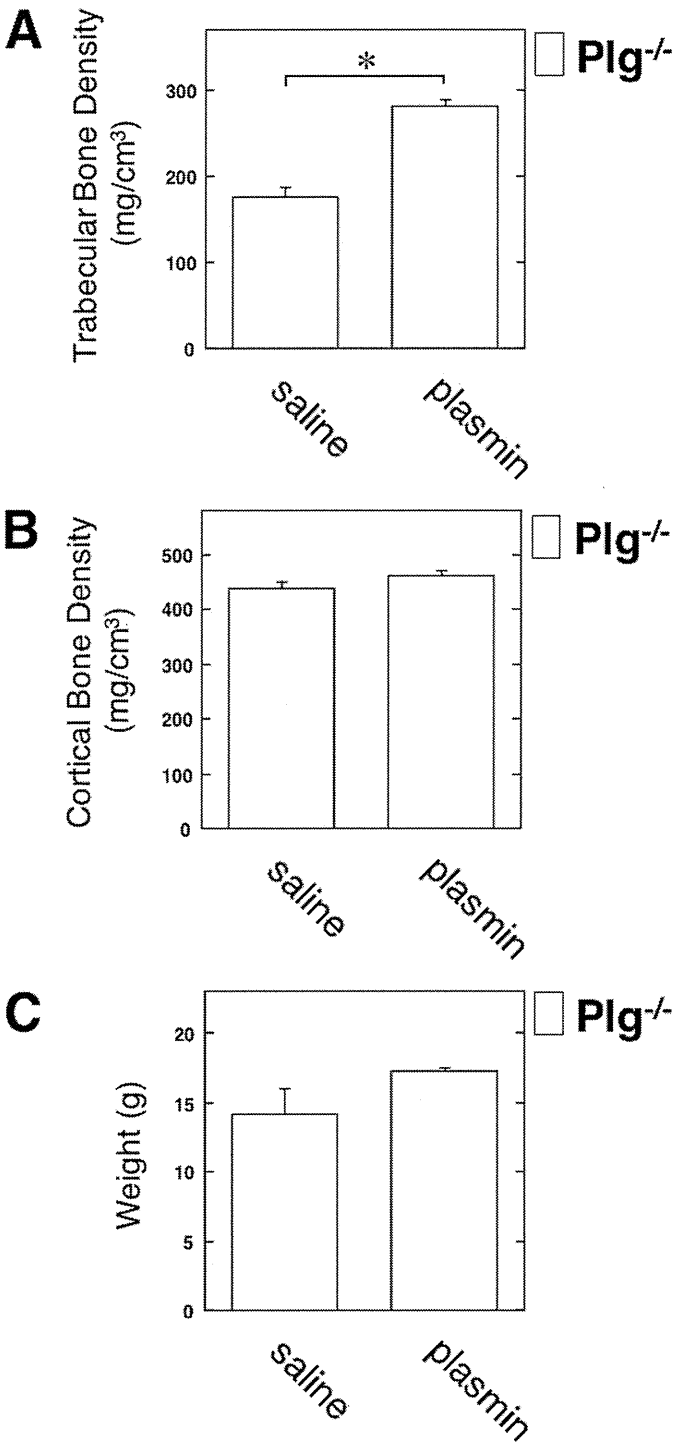

FIGURE 6. **Rescue of the down-regulated BMD in Plg-deficient mice by the injection of plasmin.** Intraperitoneal injection with saline or plasmin (1 mg/kg) in the 5-week-old male $Plg^{-/-}$ mice was carried out weekly for up to 3 weeks. Then the trabecular BMD (*A*), the cortical BMD (*B*), and the weight (*C*) in the male $Plg^{-/-}$ mice were measured by pQCT ($n = 3$). The data represent the mean ± S.E. *, $p < 0.01$.

Plasmin activates a latent transforming growth factor β (TGF-β) (24, 25) trapped in extracellular matrix to induce an OPG expression in extracellular matrix-harbored OBs. The accelerated expression of OPG on OBs might result in the suppression of the OB-mediated osteoclastogenesis. It is under investigation by us whether deficiency of activated TGF-β causes decreased bone mineral density and decreased body weight in $Plg^{-/-}$ mice. However, plasmin directly activates various intracellular signaling through annexin A2 in macrophage (26). Plasmin activates macrophages via the annexin A2 heterotetramer composed of annexin A2 and S100A10 with subsequent stimulation of Janus kinase JAK1/TYK2 signaling. JAK1/TYK2 leads to STAT3 activation, Akt-dependent nuclear factor-κB (NF-κB) activation, and phosphorylation of ERK1/2 and p38 MAPK. Furthermore, inhibitors of JAK, p38 MAPK, and NF-κB revealed that these signaling pathways are indispensable for the plasmin-mediated tumor necrosis factor-α and IL-6 induction in the cells. In addition, angiostatin, a fragment of plasmin(ogen), is a ligand and an antagonist for integrin α9β1 (27). Angiostatin, representing the kringle domains of plasmin, alone did not induce the migration of Chinese hamster ovary (CHO) cells, but simultaneous activation of the G protein-coupled protease-activated receptor-1 with an agonist peptide induced the migration on angiostatin. These facts suggest that plasmin directly stimulates various cell lineages without an indirect cell stimulation through an activation of some growth factors such as TGF-β. We showed that plasmin activated ERK1/2 and p38 MAPK, and the inhibition of ERK1/2 and p38 MAPK attenuated plasmin-induced OPG expression (Fig. 3, *E* and *F*). In addition, plasmin activated JNK, but the inhibition of JNK did not attenuate plasmin-induced OPG expression (data not shown). These data suggest that plasmin induces OPG expression through the ERK1/2 and p38 MAPK pathways. However, the time lag between the activation of p38 MAPK and ERK1/2 after plasmin stimulation in OBs might depend on the hierarchy of ERK1/2 and p38 MAPK in the plasmin-induced signal transduction. The ERK1/2 might be the downstream target of p38 MAPK directly activated by plasmin in OBs. Further investigations would be required to clarify the details.

These results strongly suggest that the plasmin activity regulates both OB and OC functions and then plays an important role in bone metabolism. These findings may provide new insights into the development of clinical therapies for the prevention of bone loss-related disorders.

REFERENCES

1. Braaten, J. V., Handt, S., Jerome, W. G., Kirkpatrick, J., Lewis, J. C., and Hantgan, R. R. (1993) *Blood* **81,** 1290–1299
2. Lijnen, H. R., De Cock, F., Van Hoef, B., Schlott, B., and Collen, D. (1994) *Eur. J. Biochem.* **224,** 143–149
3. Carmeliet, P., and Collen, D. (1996) *Semin. Thromb. Hemost.* **22,** 525–542
4. Matsuno, H., Ishisaki, A., Nakajima, K., Okada, K., Ueshima, S., Matsuo, O., and Kozawa, O. (2003) *Blood* **102,** 3621–3628
5. Kanno, Y., Kuroki, A., Minamida, M., Kaneiwa, A., Okada, K., Tomogane, K., Takeuchi, K., Ueshima, S., Matsuo, O., and Matsuno, H. (2008) *Thromb. Res.* **123,** 336–341
6. Kanno, Y., Hirade, K., Ishisaki, A., Nakajima, K., Suga, H., Into, T., Matsushita, K., Okada, K., Matsuo, O., and Matsuno, H. (2006) *J. Thromb. Haemost.* **4,** 1602–1610
7. Kanno, Y., Kuroki, A., Okada, K., Tomogane, K., Ueshima, S., Matsuo, O., and Matsuno, H. (2007) *J. Thromb. Haemost.* **5,** 2266–2273
8. Kanno, Y., Kaneiwa, A., Minamida, M., Kanno, M., Tomogane, K., Takeuchi, K., Okada, K., Ueshima, S., Matsuo, O., and Matsuno, H. (2008) *J. Invest. Dermatol.* **128,** 2792–2797
9. Kanno, Y., Kawashita, E., Minamida, M., Kaneiwa, A., Okada, K., Ueshima, S., Matsuo, O., and Matsuno, H. (2010) *Am. J. Pathol.* **176,** 238–245
10. Daci, E., Everts, V., Torrekens, S., Van Herck, E., Tigchelaar-Gutterr, W.,

Bouillon, R., and Carmeliet, G. (2003) *J. Bone Miner. Res.* **18,** 1167–1176
11. Daci, E., Verstuyf, A., Moermans, K., Bouillon, R., and Carmeliet, G. (2000) *J. Bone Miner. Res.* **15,** 1510–1516
12. Furlan, F., Galbiati, C., Jorgensen, N. R., Jensen, J. E., Mrak, E., Rubinacci, A., Talotta, F., Verde, P., and Blasi, F. (2007) *J. Bone Miner. Res.* **22,** 1387–1396
13. Wada, T., Nakashima, T., Hiroshi, N., and Penninger, J. M. (2006) *Trends Mol. Med.* **12,** 17–25
14. Hofbauer, L. C., and Heufelder, A. E. (2001) *J. Mol. Med.* **79,** 243–253
15. Li, J., Sarosi, I., Yan, X. Q., Morony, S., Capparelli, C., Tan, H. L., McCabe, S., Elliott, R., Scully, S., Van, G., Kaufman, S., Juan, S. C., Sun, Y., Tarpley, J., Martin, L., Christensen, K., McCabe, J., Kostenuik, P., Hsu, H., Fletcher, F., Dunstan, C. R., Lacey, D. L., and Boyle, W. J. (2000) *Proc. Natl. Acad. Sci. U.S.A.* **97,** 1566–1571
16. Ploplis, V. A., Carmeliet, P., Vazirzadeh, S., Van Vlaenderen, I., Moons, L., Plow, E. F., and Collen, D. (1995) *Circulation* **92,** 2585–2593
17. Suda, T., Jimi, E., Nakamura, I., and Takahashi, N. (1997) *Methods Enzymol.* **282,** 223–235
18. Kanazawa, S., Ota, S., Sekine, C., Tada, T., Otsuka, T., Okamoto, T., Sønderstrup, G., and Peterlin, B. M. (2006) *Proc. Natl. Acad. Sci. U.S.A.* **103,** 14465–14470
19. Nishiwaki, T., Yamaguchi, T., Zhao, C., Amano, H., Hankenson, K. D., Bornstein, P., Toyama, Y., and Matsuo, K. (2006) *J. Bone Miner. Res.* **21,** 596–604
20. Kanno, Y., Into, T., Lowenstein, C. J., and Matsushita, K. (2008) *Cardiovasc. Res.* **77,** 221–230
21. Nakashima, T., Kobayashi, Y., Yamasaki, S., Kawakami, A., Eguchi, K., Sasaki, H., and Sakai, H. (2000) *Biochem. Biophys. Res. Commun.* **275,** 768–775
22. Daci, E., Udagawa, N., Martin, T. J., Bouillon, R., and Carmeliet, G. (1999) *J. Bone Miner. Res.* **14,** 946–952
23. Everts, V., Daci, E., Tigchelaar-Gutter, W., Hoeben, K. A., Torrekens, S., Carmeliet, G., and Beertsen, W. (2008) *Bone* **43,** 915–920
24. Thirunavukkarasu, K., Miles, R. R., Halladay, D. L., Yang, X., Galvin, R. J., Chandrasekhar, S., Martin, T. J., and Onyia, J. E. (2001) *J. Biol. Chem.* **276,** 36241–36250
25. Lyons, R. M., Gentry, L. E., Purchio, A. F., and Moses, H. L. (1990) *J. Cell Biol.* **110,** 1361–1367
26. Li, Q., Laumonnier, Y., Syrovets, T., and Simmet, T. (2007) *Arterioscler. Thromb. Vasc. Biol.* **27,** 1383–1389
27. Majumdar, M., Tarui, T., Shi, B., Akakura, N., Ruf, W., and Takada, Y. (2004) *J. Biol. Chem.* **279,** 37528–37534

IAI Accepts, published online ahead of print on 16 April 2012
Infect. Immun. doi:10.1128/IAI.06098-11

Title: E-selectin Mediates *Porphyromonas gingivalis* Adherence to Human Endothelial Cells.

Running Title: *P. GINGIVALIS* INTERACTS WITH E-SELECTIN.

Authors: Toshinori Komatsu,[1, 2] Keiji Nagano,[3] Shinsuke Sugiura,[1] Makoto Hagiwara,[1] Naomi Tanigawa,[1] Yuki Abiko,[3] Fuminobu Yoshimura,[3] Yasushi Furuichi,[2] and Kenji Matsushita[1, 2]*

Departments of Oral Disease Research, National Center for Geriatrics and Gerontology at Obu, Aichi 474-8511, Japan, [1] Department of Periodontology and Endodontology, School of Dentistry, Health Sciences University of Hokkaido, Ishikari, Hokkaido 061-0293, Japan, [2] Department of Microbiology, School of Dentistry, Aichi-Gakuin University, Nagoya, Aichi 464-8651, Japan[3]

*Corresponding author. Mailing address: Department of Oral Disease Research, National Institute for Longevity Science, National Center of Geriatrics and Gerontology, Obu, Aichi 747-8511, Japan. Phone: +81-562-46-2311. Fax: +81-562-46-8479. E-mail: kmatsu30@ncgg.go.jp

ABSTRACT

Porphyromonas gingivalis, a major periodontal pathogen, may contribute to atherogenesis and other inflammatory cardiovascular diseases. However, little is known about interactions between *P. gingivalis* and endothelial cells. E-selectin is a membrane protein on endothelial cells that initiates recruitment of leukocytes to inflamed tissue, and it may also play a role in pathogen attachment. In the present study, we examined the role of E-selectin in *P. gingivalis* adherence to endothelial cells. Human umbilical vein endothelial cells (HUVECs) were stimulated with TNF-α to induce E-selectin expression. Adherence of *P. gingivalis* to HUVECs was measured by fluorescent microscopy. TNF-α increased adherence of wild-type *P. gingivalis* to HUVECs. An antibody to E-selectin and sialyl Lewis X suppressed *P. gingivalis* adherence to stimulated HUVECs. *P. gingivalis* mutants lacking OmpA-like proteins Pgm6/7 had reduced adherence to stimulated HUVECs, but fimbriae-deficient mutants were not affected. E-selecin-mediated *P. gingivalis* adherence activated endothelial exocytosis. These results suggest that the interaction between host E-selectin and pathogen Pgm6/7 mediates *P. gingivalis* adherence to endothelial cells and may trigger vascular inflammation.

Key Words: periodontitis, atherogenesis, outer membrane protein, vascular inflammation

INTRODUCTION

Periodontitis is a disease of the supporting structures of the teeth, causing loss of attachment to the alveolar bone and eventual exfoliation of teeth (5). Severe periodontitis affects up to 20% of the population, and mild-to-moderate periodontitis is observed in the majority of adults (6). Gram-negative bacteria play an important role in the pathogenesis of human periodontal diseases (15) (42) and *Porphyromonas gingivalis* is one of the species most strongly implicated in periodontal diseases (14) (43). Several recent studies have demonstrated that *P. gingivalis* is able to invade and activate different cell types in the tissue surrounding teeth (endothelial and gingival epithelial cells as well as periodontal ligament cells) (12) (26) (40). Moreover, recent studies have demonstrated a transient bacteremia with potential systemic infection after a variety of dental treatment procedures (2) (19) (20) (41). Endothelial cells, therefore, can act as primary target cells during infection with *P. gingivalis*. However, little is known about mechanisms of infection and activation of endothelial cells by *P. gingivalis*.

The endothelium has several important functions that include providing a nonadhesive, nonthrombotic barrier between the blood and the underlying tissues. In atherosclerosis, or in response to injury or inflammatory cytokines such as tumor necrosis factor α (TNF-α), the endothelium becomes activated and selectins and cell adhesion molecules (CAMs) are rapidly induced (39) (36). In particular, members of the immunoglobulin superfamily of CAMs, such as intercellular cell adhesion molecule-1 (ICAM-1) and vascular cell adhesion molecule-1 (VCAM-1), as well as selectin family members, E-selectin and P-selectin, are expressed and play crucial roles in the adhesion and migration of monocyte/macrophage infiltration into atherosclerotic lesions during the early and subsequent stages of atherosclerosis in a variety of animal models (47) (21) (49). Increased expression of E-selectin and production of pro-inflammatory cytokines in the

endothelium play a pivotal role in the generation of leukocyte infiltrates and subsequent atherosclerotic plaque formation (28) (16). *P. gingivalis* infection significantly increases endothelial expression of VCAM-1, ICAM-1 and E-selectin, enhances production of IL-6, IL-8 and MCP-1, and increases adhesion of THP-1 monocytes to endothelial cells (46) (18) . Therefore, *P. gingivalis* elicits a pro-atherogenic response in endothelial cells. Although E-selectin is involved in vascular inflammation and is induced with *P. gingivalis*, interaction between *P. gingivalis* and endothelial cells is not understood. In the present study, we explored the ability of E-selectin to facilitate *P. gingivalis a*dherence to human umbilical vein endothelial cells (HUVECs). We found that activated endothelial cells interact with *P. gingivalis* via E-selectin on endothelial cells and via OmpA-like proteins Pgm6/7 of the bacteria.

MATERIALS AND METHODS

Bacterial strains and growth conditions. *P. gingivalis* ATCC 33277 was used as a wild-type strain in this study. *P. gingivalis* defective mutants lacking *fimA* were constructed as described previously (17). A *P. gingivalis* Pgm6/7-deficient mutant was constructed as described previously (32). This mutant did not show any sign of a polar effect on the downstream gene (data not shown). All *P. gingivalis* strains were grown at 37 ℃ under anaerobic conditions (10% CO_2, 10% H_2, and 80% N_2) on *Brucella* HK agar (Kyokuto Pharmaceutical Industrial Co., Ltd., Tokyo, Japan) supplemented with 5% laked rabbit blood, haemin (2.5 μg/ml), menadione (5 μg/ml) and dithiothreitol (0.1 mg/ml) and in trypticase soy broth (BD, Franklin Lakes, NJ) supplemented with yeast extract (2.5 mg/ml), haemin (2.5 μg /ml), menadione (5 μg/ml) and dithiothreitol (0.1 mg/ml). Bacterial growth was monitored by measuring OD_{660}. For infection assays, an infection ratio (multiplicity of infection) of 100 bacteria per cell was added to the cell culture medium.

Cell culture conditions. Human umbilical vein endothelial cells (HUVECs) were cultured in endothelial cell growth medium-2 (EGM-2) (Lonza, Basel, Switzerland) supplemented with fetal bovine serum, hydrocortisone, human recombinant fibroblast growth factor, vascular endothelial growth factor, recombinant insulin growth factor-1, ascorbic acid, human recombinant epidermal growth factor, gentamicin, and amphotericin B at 37℃ in an atmosphere of 5% CO_2. Cells were cultured in 75-cm^2 flasks at 37°C in a humidified atmosphere of 5% CO_2. Both HCAECs and CASMCs were cryopreserved at the third passage and were passaged an additional two or three times before use.

E-selectin expression. E-selectin cDNA was constructed as described previously (53). The E-selctin cDNA was amplified by PCR with specific primers (5'-gac agc tag cat gat tgc ttc aca g-3', including an additional Nhe site, and 5'-cgg cct cga gtt aaa gga

tgt aag aag gc-3', including an additional Xho site) and cloned into pcDNA3.1 vector (Invitrogen, Carlsbad, CA). For preparation of a soluble E-selectin vector, a stop codon and unique EcoRV site were introduced by site-directed mutagenesis (Promega, Madison, WI) into the boundary between the sixth consensus repeat and the transmembrane domain using the following oligonucleotide, which starts at nucleotide 1776: 5"CC AAC ATT CCC TAG ATA TCT AGA CTT TCT GCT G-3'.

Measurement of E-selectin production. An ELISA-based method was used for quantification of E-selectin protein expression in endothelial cells. HUVECs (3.5×10^5 cells/ml) were seeded into 6-well plates and grown overnight. Then the cells were stimulated with 10 ng/ml of TNF-α (PeproTec Inc., Rocky Hill, NJ) for 1, 2, 3, 4, 8, and 24 h. After removing the media, the cell layers were washed twice with PBS. Cells were lysed in a cell lysis reagent (CelLytic P, Sigma-Aldrich, St. Louis, MO) with protease inhibitor mixture (Nacalai Tesque, Kyoto, Japan). Concentrations of E-selectin in the cell lysates were determined using a commercial ELISA kit for E-selectin (eBioscience, San Diego, CA). The cell lysates were also mixed with 4x Laemmli sample buffer without reducing agents and were fractionated on a 7.5% SDS-PAGE and immunoblotted with a monoclonal antibody to E-selectin (BBIG-E4 (5D11): R&D Systems, Abingdon, U.K.).

Analysis of *P. gingivalis* adhesion to endothelial cells. HUVECs (2×10^6 cells) were seeded in a Lab-Tek II Chamber Slide System (Nalge Nunc International, Rochester, NY) that has been coated with 50 mg/ml of rat tail collagen (BD) and the cells were incubated for 24 h before administration of *P. gingivalis*. HUVECs grown to near confluence per well were stimulated with TNF-α for 3 h and then *P. gingivalis* cells, which had been washed with EGM-2 and resuspended in EGM-2 without an antibiotic at a concentration of 10^8 cells/ml, were added to the monolayer cells at an MOI of 1:100 under 5% CO2 at 37℃ for 0.5-3 h. Cells were then washed three times with PBS, followed

each time by gentle rinsing for 5 min at room temperature, and fixed with 4% (w/v) paraformaldehyde at 4℃ overnight. After washing three times with PBS, the cells were permeabilized with PBS containing 0.05% Triton-X-100 at room temperature for 30 min. They were washed again and then blocked with PBS containing 5% (w/v) BSA at room temperature for 30 min. Bacterial cells on chamber slides were labeled with an antiserum for *P. gingivalis* whole-cells (1: 1000 dilution) for 60 min at room temperature and washed five times with PBS. Then the bacterial cells were incubated with Alexa Fluor 488 goat anti-rabbit IgG (1:1000 dilution, Invitrogen Co., Carlsbad, CA). Actin filaments in HUVECs or 293 cells were simultaneously stained with Alexa Fluor 568 phalloidin (1 μg/ml, Invitorgen Co.) for 60 min at room temperature in the dark. After washing 10 times with PBS, chamber slides were mounted onto a slide containing ProLong Gold antifade reagent (Invitrogen). Adherent bacteria on the cell surface were examined by fluorescent microscopy (Keyence, Osaka, Japan). We measured the area stained with Alexa488 (corresponding to *P. gingivalis*) in a visual field (corresponding to 0.06 mm^2) by using Image J program. We then calculated bacterial number by dividing the area by the size (pixel) of a *P. gingivalis* cell. To determine whether E-selectin is involved in *P. gingivalis* adherence to endothelial cells, TNF-α-pretreated HUVECs were incubated with *P. gingivalis* ATCC 33277 (10^8 cells/ml/well) for 30 min-3 h in the presence of various concentrations of an antibody for E-selectin (R&D Systems, Inc., Minneapolis, MN), recombinant E-selectin, and Sialyl Lewis X (Calbiochem, San Diego, CA). *P. gingivalis* ATCC 33277 (10^8 cells/ml/well) was also incubated with HEK 293 cells transfected with a human E-selectin-inserted vector for 30 min. To explore ligands for E-selctin on *P. gingivalis*, *P. gingivalis* ATCC 33277 (wild type), FimA-deficient mutant (Δ*fimA*), and Pgm6/7-deficient mutant (Δ*pgm6/7*) (10^8 cells/ml) were incubated with TNF-α-pretreated HUVECs for 3 h, respectively. TNF-α-pretreated HUVECs were incubated with *P.*